ARTICLE | OPEN ACCESS

**Drug Discovery**

# In Vitro Evaluation and Molecular Docking Studies of α-Glucosidase and α-Amylase Inhibitory and Antioxidant Activities of *Anacardium occidentale* Leaves

**Tajudeen Afolayan Lawal***

**To Cite:**
Lawal TA. In Vitro Evaluation and Molecular Docking Studies of α-Glucosidase and α-Amylase Inhibitory and Antioxidant Activities of *Anacardium occidentale* Leaves. *Drug Discovery* 2026; 20: e19dd3107 doi:

**Author Affiliation:**
Biochemistry and Forensic Science Department, Faculty of Science, Nigeria Police Academy, Wudil, Kano, Nigeria

***Corresponding Author:**
Tajudeen Afolayan Lawal,
Biochemistry and Forensic Science Department, Faculty of Science, Nigeria Police Academy, Wudil, Kano, Nigeria,
Email: lawalat40@gmail.com; talawal@polac.edu.ng

**Peer-Review History**
Received: 12 March 2026
Reviewed & Revised: 27/March/2026 to 21/September/2026
Accepted: 30 September 2026
Published: 09 October 2026

**Peer-Review Model**
External peer-review was done through double-blind method.

Drug Discovery
pISSN 2278–540X; eISSN 2278–5396

© The Author(s) 2026. Open Access. This article is licensed under a Creative Commons Attribution License 4.0 (CC BY 4.0)., which permits use, sharing, adaptation, distribution and reproduction in any medium or format, as long as you give appropriate credit to the original author(s) and the source, provide a link to the Creative Commons license, and indicate if changes were made. To view a copy of this license, visit http://creativecommons.org/licenses/by/4.0/.

## ABSTRACT

The rising global prevalence of diabetes mellitus highlights the need for new plant-based therapeutic agents with both antidiabetic and antioxidant properties. The ethyl acetate subfraction (SF5) of the methanolic leaf extract of *Anacardium occidentale* was evaluated for its ability to inhibit α-amylase and α-glucosidase. The study also assessed its antioxidant activity, phytochemical composition, and predicted molecular interactions. The fractions were evaluated using in vitro enzyme-inhibition and antioxidant assays. At the same time, the phytoconstituents of the most potent subfraction were characterized by LC-MS. The methanolic extract of *Anacardium occidentale* leaves (MEAOL) was fractionated by column chromatography to obtain pooled fractions (PF1 to PF8). PF5 exhibited the strongest enzyme-inhibitory activity and was further fractionated into six subfractions (SF1 to SF6). SF5 exhibited the strongest antidiabetic and antioxidant activities among the subfractions tested. The $IC_{50}$ of SF5 for α-amylase inhibition is 23.84±2.42 µg/mL, for α-glucosidase inhibition is 19.54±1.05 µg/mL, for DPPH radical scavenging activity is 28.63±1.78 µg/mL, and for metal chelating activity is 21.87±1.92 µg/mL. The result of FTIR analysis indicates the presence of phenolic, hydroxyl, and carbonyl functionalities. These functional groups are commonly associated with antidiabetic and antioxidant bioactive compounds. The LC-MS analysis results revealed the presence of gallic acid, protocatechuic acid, methyl gallate, methyl ursolate, quercetin-3-O-arabinose, luteolin-7-O-glucoside, and amentoflavone. These compounds are composed of biologically active compounds such as phenolic acids, flavonoids, and triterpenoids. Molecular docking was used to assess the affinities and interactions between the compounds and the target proteins. Luteolin-7-O-glucoside (-6.91 kcal/mol), quercetin-3-O-arabinoside (-6.26 kcal/mol), and amentoflavone (-7.11 kcal/mol) showed favorable interactions with important residues of α-amylase and α-glucosidase, compared with the reference inhibitor acarbose (-8.47 and -7.09 kcal/mol, respectively). Hydrogen bonds involving His299, Asp300, Glu233, and Asp443 were observed in the docked complexes, indicating possible contributions to enzyme inhibition. The compounds also showed binding affinities of −7.26 to −7.10 kcal/mol toward HO-1, which were consistent with the antioxidant activity observed in vitro.

Generally, the results indicate that the SF5 fraction of *Anacardium occidentale* leaves has antidiabetic and antioxidant activities. The activity may be associated, at least in part, with its polyphenolic and flavonoid constituents. The results provide evidence for the potential *of Anacardium occidentale* leaves as a source of compounds with enzyme-inhibitory and redox-related activities. Further work involving enzyme kinetics, mechanistic studies, and in vivo models would be useful for establishing the mechanisms underlying these activities and evaluating the prospects for phytotherapeutic formulation.

**Keywords:** *Anacardium occidentale*, α-amylase, α-glucosidase, antioxidant, molecular docking, LC-MS, HO-1

## 1. INTRODUCTION

Diabetes mellitus (DM) is a long-term metabolic disease characterized by abnormally high blood glucose (blood sugar). It occurs when the body either does not produce enough insulin, does not respond properly to insulin (insulin resistance), or both (Dirir et al., 2022). There are three common types of DM. They are: type 1 diabetes mellitus (T1DM), type 2 diabetes mellitus (T2DM), and gestational diabetes (GD). The T1DM is caused by autoimmune destruction of pancreatic β-cells, which leads to little or no insulin production. The T2DM involves insulin resistance and a gradual decline in insulin secretion. The GD is developed during pregnancy (Dirir et al., 2022). The T2DM has been significantly reported in morbidity and mortality worldwide. The control of the rise in blood glucose after a carbohydrate meal (postprandial hyperglycemia) is an important aspect of diabetes management. Prolonged postprandial hyperglycemia has been linked to diabetes complications (Lawal et al., 2022). α-Amylase and α-glucosidase are hydrolytic enzymes that help to digest dietary carbohydrates. When these enzymes are inhibited, the carbohydrate digestion may be delayed, which may ultimately cause moderation in postprandial hyperglycemia (Pan et al., 2024). The common drug used to control postprandial hyperglycemia is acarbose. This drug is clinically designed as an α-glucosidase inhibitor. However, this drug worked with adverse gastrointestinal effects. Because of these adverse effects, there is a need to search for natural enzyme inhibitors that are safer (Kashtoh & Baek, 2022).

Reports have shown that plant-derived metabolites such as polyphenols, flavonoids, phenolic acids, tannins, and terpenoids have α-amylase and α-glucosidase inhibiting activities (Assefa et al., 2020; Kashtoh & Baek, 2022). These compounds have been shown to have appreciable α-glucosidase inhibitory activity in vitro, which is comparable with those of standard or synthetic conventional antidiabetic agents (Dirir et al., 2022). These metabolites have also been shown to exhibit antioxidant activities against oxidative stress linked to diabetes and its complications (Etsassala et al., 2022). The prevalence of both enzyme inhibitory and antioxidant properties within the same plant-derived compound is of interest in the search for antidiabetic agents, such as compounds acts at different stages involved in postprandial glucose regulation and oxidative damage. This makes plant metabolites useful candidates for further investigation (Ali et al., 2023; Etsassala et al., 2022).

*Anacardium occidentale* L., which is known as Cashew in English, has been used widely in traditional medication in the management of diabetes in Tropical regions. The parts of this plant commonly used include leaves, bark, etc which have been reported to contain phytochemicals such as anacardic acid tannins, gallic acid derivatives, and polyphenolic compounds (Encarnacao et al., 2022). Anacardic acid and other phenolic compounds have been linked to α-amylase and α-glucosidase inhibitory activities (Silva et al., 2024).

The biological activity of plant extracts and fractions can be examined using in vitro enzyme assays and antioxidant tests. α-Glucosidase and α-amylase inhibition assays, along with DPPH, ABTS, FRAP, and measurements of total phenolic and flavonoid contents, are commonly used for preliminary screening of such samples (Oyedemi et al., 2017). Molecular docking has been found to complement the laboratory testing by modelling how the detected phytochemicals may interact with the target enzymes. In this regard, the predicted binding modes and affinities can be interpreted together with the in vitro results to assess the contribution of each compound (Rangel-Galvan et al., 2024). Combinations of these methods are to offer an early-stage strategy for screening plant-based compounds with both antidiabetic and antioxidant potential activities.

Leaf extracts of *Anacardium occidentale* have shown antidiabetic and antioxidant activities, but how each fraction and its constituents relate to enzyme inhibition remains unclear (Konare et al., 2024; Lawal et al., 2024). There is limited information on how compounds from specific fractions interact with relevant target enzymes. Further work to compare the enzyme inhibitory activity of different leaf fractions with the predicted binding of their detected compounds. Comparing these predictions with the established inhibitors (standard drugs) may help to interpret the experimental results

The present study evaluated the solvent fractions of methanolic leaf extract of *Anacardium occidentale* (MEAOL) for α-glucosidase and α-amylase inhibitory activities and antioxidant capacity using standard in vitro assays. Active fractions are subjected to phytochemical analysis to identify their principal constituents, followed by molecular docking of selected compounds with α-glucosidase and α-amylase. The combined experimental and computational approaches are used to examine the potential of Anacardium occidentale leaf constituents as natural inhibitors relevant to the control of postprandial hyperglycemia.

## 2. MATERIALS AND METHODS

### 2.1. Sample Collection and Preparation

Cashew leaves (*Anacardium occidentale*) were collected from the Botanical Garden of the Department of Biological Sciences, Bayero University Kano (BUK), Kano State. Dr. Yusuf Nuhu, a plant taxonomist in the department herbarium section, identified and authenticated the leaf and assigned it accession number BUKHAN0413. The leaves were washed with deionized water and shade-dried for two weeks until a constant weight was reached. The dried leaves were ground with a mortar and pestle. Then, 50 g of the powder was soaked in 500 mL of methanol for 72 hours, with intermittent shaking. The mixture was filtered through mesh cloth and Whatman Grade 1 filter paper. The filtrate was subsequently evaporated in a water bath at 40 °C until a solid crude extract was formed. The extract was then placed in a labeled plastic container marked "Methanol Extract of *Anacardium occidentale* Leaves (MEAOL)" and stored until further use.

### 2.2. Fractionation

**(a) Column Chromatography**

Silica gel (120 G mesh) was used as the stationary phase, and different solvent combinations were used as eluents. The column was packed with 200 g of silica gel suspended in 500 mL of hexane. The tap was then opened to allow the solvent to drain into a beaker placed beneath the column. After packing, the tap was closed, and the apparatus was left undisturbed for 24 hours. The clear solvent above was drained to the level of the silica gel meniscus, and the column's flow rate was measured. Five grams (5 g) of the dried MEAOL were thoroughly mixed with 10 g of silica gel and then gently spread onto the top of the column. The column was eluted sequentially with solvent mixtures of increasing polarity. The column was eluted with hexane and ethyl acetate mixtures at the following ratios: 100:0, 90:10, 80:20, 70:30, 60:40, 50:50, 40:60, 30:70, 20:80, 10:90, and 0:100. Each solvent system was applied until the eluate became clear. The eluents were collected in 50 mL portions.

**(b) Thin Layer Chromatography, TLC (Analytical)**

The fractions obtained from column chromatography were merged using analytical thin-layer chromatography (TLC). Each fraction was applied onto a pre-coated aluminum silica gel plate (Macherey-Nagel, Germany, 2023) and developed in a glass chromatographic chamber with methanol as the solvent. A sample was spotted 1.0 cm above the bottom edge of the plate, which was then dried before placement in a solvent-saturated chamber. The solvent ascended the plate until it reached about three-quarters of the way up, then dried again. The TLC plate was sprayed with a reagent containing *p*-anisaldehyde, glacial acetic acid, and sulfuric acid and then heated at 105 °C for 10 seconds to develop the spots. The colors of the spots were recorded, and the corresponding retention factor (Rf) values were determined. Fractions showing similar spot patterns and Rf values were combined. Each pooled fraction was then tested for antioxidant activity and for inhibition of α-amylase and α-glucosidase.

### 2.3. Assessment of Enzyme Inhibition Potentials

**(a) Screening for α-Glucosidase Inhibition**

The inhibitory effects of each fraction and sub-fraction on α-glucosidase activity were evaluated using the protocol described by Dej-Adisai (2021), with slight modifications. Different concentrations of the fractions (10, 30, 60, and 80 µg/mL) were prepared in 20 mM sodium phosphate buffer (pH 6.9).

For each fraction, 100 µL of the test solution was added to 100 µL of α-glucosidase solution (1.0 U) and incubated at 37 °C for 10 minutes. Next, 100 µL of 10 mM p-NPG was added, and the mixture was incubated at 37 °C for 10 minutes further. The reaction was put to stop with addition of 5 mL of 20 mM $Na_2CO_3$. The absorbance of the mixture was then taken at 405 nm. The process was repeated without the fraction (using only the buffer as a negative control). A positive control was also performed, replacing the fraction with the

standard acarbose medication. The absorbance readings were converted to the amount of p-nitrophenol released using a standard curve for p-nitrophenol. Enzyme activity was calculated using the formula in Equation 1.

$$\text{A unit of α-glucosidase activity} = \frac{Mg_{pNP} \times DF}{T \times Mg_{EzG}} \quad ...Equation\ 1$$

Where $Mg_{pNP}$ denotes the mg of p-nitrophenol released, DF refers to the factor by which the mixture is diluted, T signifies the time of the reaction, and $Mg_{EzG}$ indicates the mg of the enzyme ($\alpha$-glucosidase) in the reaction mixture.

The percentage of $\alpha$-glucosidase activity was calculated using Equation 2.

$$\text{α-glucosidase activity}(\%) = \frac{In_A}{Un_A} \times 100 \quad ....Equation\ 2$$

$In_A$ represents the inhibited enzyme activity, and $Un_A$ represents the activity of the uninhibited enzyme.

To determine the concentration of each fraction required to inhibit enzyme activity by 50% ($IC_{50}$), percentage enzyme activity was plotted against fraction concentration. The fraction with the lowest $IC_{50}$ was analyzed using LC-MS techniques to identify its components.

**(b) Screening for $\alpha$-Amylase inhibitor**

The slightly modified method of Lawal et al. (2024) was used for this assay. Sodium phosphate buffer (20 mM; pH 6.9) was used to dissolve fractions and subfractions. Concentrations of 0.08, 0.16, 0.24, 0.32, and 0.40 mg/mL were then prepared. Exactly 100 µL of each concentration was added to 250 µL of $\alpha$-amylase solution (0.5 mg/mL) and then incubated at 25 °C for 10 minutes. Into the mixture 250 µL of 1% starch solution was added. The mixture was then incubated for another 10 minutes at 25 °C. DNSA (500 µL) was added to stop the reaction. Thereafter, the mixture was heated in boiling water for 5 minutes, then cooled to room temperature. The mixture was diluted to 10 mL with distilled water. The absorbance of the mixture was measured at 540 nm.

For the negative control, buffer was used to replace the test sample. Acarbose was used as positive control, and they were all tested at the same concentrations. For the reagent blank, buffer solution was used to replace the $\alpha$-amylase solution to account for background absorbance. Maltose released during the reaction was determined using a maltose calibration curve. The $\alpha$-amylase activity was subsequently determined using Equation 3.

$$\text{A unit of α-amylase activity} = \frac{Mg_m \times DF}{T \times Mg_{EzA}} \quad ...Equation\ 3$$

Where $Mg_m$ denotes the mg of maltose released, DF refers to the factor by which the mixture is diluted, T signifies the time period of the reaction, and $Mg_{EzA}$ indicates mg of the enzyme ($\alpha$-amylase) in the reaction mixture.

The percentage of enzyme activity was calculated using Equation 4.

$$\text{α-amylase activity}(\%) = \frac{In_A}{Un_A} \times 100 \quad ....Equation\ 4$$

$In_A$ represents the inhibited enzyme activity, while $Un_A$ represents the activity of the uninhibited enzyme.

A graph of percentage enzyme activity versus fraction concentration was plotted. This enabled determination of the concentration required to reduce enzyme activity by 50% ($IC_{50}$). The fraction with the highest potency, indicated by the lowest $IC_{50}$, underwent further analysis using LC-MS methods to identify its components.

**2.4. Antioxidant Potential Assays**

**(a) DPPH Radical Scavenging Assay**

The DPPH radical scavenging activity assay of the fraction was carried out according to the method of Baliyan et al. (2022), with minor modification. The fractions were dissolved in methanol at concentrations of 100 – 600 µg/mL. Into each 2 mL concentration of the fraction, 2 mL of freshly prepared 0.1 mM DPPH solution was added. The mixture was kept in a dark cupboard at room temperature for 30 minutes. The absorbance was then measured at 517 nm.

DPPH solution without a fraction served as the negative control, and methanol served as the blank. Ascorbic acid in place of the fraction served as the positive control. The percentage reduction in absorbance relative to the negative control was used to determine the radical scavenging activity. DPPH radical scavenging activity (RSA) was expressed as percentage inhibition, using Equation 5.

$$\% \text{ RSA} = \frac{A_{NC} - A_T}{A_{NC}} \times 100 \qquad \ldots \textit{equation } 5$$

Where $A_{NC}$ refers to the absorbance of the negative control, whereas $A_T$ refers to the absorbance obtained for each test fraction or positive control.

Percentage inhibition was plotted against fraction concentration to produce concentration-response curves. The $IC_{50}$ was determined from each curve and represents the concentration required to reduce the DPPH radical by 50%. A lower $IC_{50}$ indicates greater scavenging activity. The fraction with the lowest $IC_{50}$ was then selected for LC-MS analysis.

**(b) Metal Chelating Properties**

$Fe^{2+}$-chelating activity of the fractions was determined according to Yadav et al. (2007) and Wong et al. (2014), with minor modifications. Briefly, 100 µL of each fraction concentration (100-600 µg/mL) was mixed with 50 µL of 2 mM ferrous chloride. The reaction was started by adding 200 µL of 5 mM ferrozine solution. The mixture was made up to a final volume of 0.8 mL with methanol and incubated for 10 minutes. Absorbance was then measured at 562 nm. EDTA (100 µL, 10 mg/L) was used as the standard or positive control. Methanol was used in place of the fraction or standard control as the negative control. For the blank, methanol was used in place of ferrozine solution. Percentage metal-chelating activity was calculated using Equation 6.

$$\% \textit{ Metal Chelation} = \frac{A_{NC} - A_T}{A_{NC}} \times 100 \quad \ldots \textit{equation } 6$$

$A_{NC}$ and $A_T$ stand for the absorbance of the negative control and test fractions, respectively. Percentage chelating activity was plotted against concentration, and $IC_{50}$ was estimated from the curve. The fraction with the lowest $IC_{50}$ indicates the greatest chelating activity. The fraction with the greatest potency was selected for further analysis.

**2.5. Preparative Thin Layer Chromatography (PTLC)**

PTLC was conducted following the method of Yadav et al. (2007). The most active pooled fraction against antidiabetic and antioxidants was subjected to PTLC. Glass plate (20 × 20 cm) was coated with silica gel slurry (1:2 w/v in water) to 0.25 mm thickness. The plate was then air-dried for 30 min and activated in an oven at 100 °C for 1 hour. Samples and standards were applied as streaks, leaving a 2.5 cm margin from one end of the plate. PTLC was carried out with chloroform and methanol in a 1:1 (v/v) ratio as the mobile phase. The developing chamber was saturated with solvent vapor for 1 hour. The plates were developed vertically until the solvent front neared the top edge. They were then removed and dried, and the bands were examined under UV light. Blue, fluorescent bands were marked, scraped off the plates, and extracted with methanol. The extracts were collected, evaporated to dryness, and quantified before further analysis.

### 2.6. Fourier Transform Infrared Spectroscopy Analysis

The Fourier Transform Infrared (FTIR) spectrum of SF5 was obtained using the KBr pellet technique with the aid of a spectrometer. The powdered sample (2 mg) was mixed with 200 mg of potassium bromide (KBr) and compressed into a transparent pellet. The instrument was checked with a polystyrene film, and a background spectrum was recorded to account for atmospheric contributions. The pellet was placed in the instrument, and its spectrum was recorded from 400 to 4500 $cm^{-1}$. The interferogram was Fourier-transformed to produce the absorbance spectrum. Absorption bands were assigned by their wavenumber regions to identify functional groups in SF5.

### 2.7. LC-MS Analysis and Compound Identification

The modified method of Piovesana et al. (2018) was used for LC-MS analysis. It was performed using a Waters e2695 separation module equipped with a PDA detector and an ACQ-QDA mass spectrometer. The fraction was dissolved in LC-MS grade methanol and filtered through a 0.45 µm PTFE membrane. A 10 µL sample was injected onto a SunFire C18 column (5.0 µm, 4.6 × 150 mm), and maintained at 25 °C with a flow rate of 1.0 mL/min. The mobile phase consisted of 0.1% formic acid in water (A) and acetonitrile (B). The mobile phase was maintained at 95:5 (A:B) for 13 minutes. It was later changed to 5:95 for 13 minutes and then returned to 95:5 for 20 minutes. The PDA detector scanned from 210 to 400 nm. Mass spectra were gotten in positive and negative electrospray ionization modes over an *m/z* range of 100–1250. The capillary voltage was 0.8 kV, and the probe temperature was 600 °C. The gas flow rate was 10 mL/min, and the nebulizer pressure was 45 psi. Data was processed using Empower 3 software.

Compounds were identified by comparing their base-peak *m/z* values with MassBank entries. They were then docked against target proteins by using MOE software.

### 2.8. Molecular Docking

The modified method of Islam et al. (2023) was used for molecular docking. Ligand and protein structures were downloaded from PubChem and the Protein Data Bank (PDB), respectively. Ligands and proteins were prepared using the method of Pham et al. (2023), with modifications. Preparation of structures started by adding hydrogen atoms and assigning charges using the MMFF94x force field. Then the structure was energy-minimized to an RMS gradient of 0.1 kcal/mol/Å.

MOE 2015 was used for docking. Ligands were placed in the AMBER14 force field, the Triangle Matcher algorithm, scored with London dG, and refined using GBVI/WSA dG. Poses of 30 were produced for each ligand. The 10 top-ranked poses were chosen using RMSD values, docking scores, and ligand–protein interactions. Docked results with favorable scores (most negative values) were chosen for further analysis.

## 3. RESULTS AND DISCUSSION

### 3.1. Results

Table 1 presents the results for the individual fractions (F1 to F30) obtained through column chromatography, along with the pooled fractions (PF1 to PF10) and the corresponding number of spots for each. Fractions with identical numbers of spots and Rf values, as determined by analytical TLC analysis, were pooled into single fractions (PF1 to PF7). The pooled fractions were evaluated for their ability to inhibit both $\alpha$-amylase and $\alpha$-glucosidase, and their antioxidant properties were also assessed.

**Table 1**. Pooled Fractions Collected from Column Chromatography

| MEAOL Fraction | Pooled Fraction | Number of Spots with Similar $R_f$ |
|---|---|---|
| **F1 – F2** | PF1 | 0 |
| **F3 – F6** | PF2 | 4 |
| **F7 – F11** | PF3 | 5 |
| **F12 – F13** | PF4 | 4 |
| **F14 – F17** | PF5 | 5 |

| | | |
|---|---|---|
| **F18 – F23** | PF6 | 2 |
| **F24 – F28** | PF7 | 3 |
| **F28 – F30** | PF8 | 2 |

Table 2 presents the results of the inhibitory effects of pooled fractions (in the form of $IC_{50}$) on α-glucosidase and α-amylase. PF5 has the lowest $IC_{50}$ values of 60.37 ± 3.24 for α-glucosidase and 32.24 ± 2.44 for α-amylase, making it the most potent fraction. PF5 was then subjected to preparative thin-layer chromatography (PTLC) analysis.

**Table 2**. $IC_{50}$ Values of Pooled Fractions

| **Pooled Fractions** | **$IC_{50}$ (μg/mL)** | |
|---|---|---|
| | α-Glucosidase | α-Amylase |
| **PF1** | - | - |
| **PF2** | 212.22±5.07 | 290.11±03.50 |
| **PF3** | 235.12±18.32 | 223.53±11.10 |
| **PF4** | 136.35±2.87 | 354.82±10.33 |
| **PF5** | **60.37±3.24** | **32.24±02.44** |
| **PF6** | 152.23±2.44 | 184.70±03.17 |
| **PF7** | 124.21±4.24 | 198.52±04.73 |
| **PF8** | 192.24±02.24 | 199.09±07.88 |

Table 3 shows the Sub-fractions (SF1 – SF6) obtained from PTLC analysis of PF5. The retardation factors ($R_f$), along with the percentage yields of each Sub-fraction, are provided. Sub-fraction 3 (SF3), with an Rf value of 0.81, had the highest percentage yield (20.60%). All the sub-fractions were evaluated for their inhibitory effects on α-glucosidase and α-amylase.

**Table 3**. Fractions Obtained From PTLC

| **Sub-fractions of PF5** | **Retardation Factor ($R_f$)** | **% Yield** |
|---|---|---|
| SF1 | 0.92 | 11.70 |
| SF2 | 0.88 | 14.90 |
| SF3 | 0.81 | 20.60 |
| SF4 | 0.76 | 18.70 |
| SF5 | 0.68 | 17.60 |
| SF6 | 0.63 | 16.50 |

Table 4 presents the bioactivity assessment of the sub-fractions, showing different degrees of enzyme inhibition and antioxidant activity. SF5 had the lowest $IC_{50}$ values across all four assays. It had 19.54 ± 1.05 μg/mL for α-glucosidase and 23.84 ± 2.42 μg/mL for α-amylase. It also had 28.63 ± 1.78 μg/mL for DPPH radical scavenging and 21.87 ± 1.92 μg/mL for metal chelation. These results are similar to the standard inhibitor, scavenger, and chelator: acarbose (α-glucosidase: 17.82 ± 1.01 μg/mL; α-amylase: 21.43 ± 1.05 μg/mL),

ascorbic acid (DPPH: 37.87 ± 1.01 µg/mL), and EDTA (metal chelation: 29.12 ± 2.31 µg/mL). SF4 and SF6 showed moderate activity, while SF1–SF3 exhibited weaker inhibitory and antioxidant effects with higher $IC_{50}$ values. Overall, SF5 was the most active fraction, suggesting that it contains compounds with notable antidiabetic and antioxidant properties. It was subsequently analyzed using FTIR and LC-MS techniques.

**Table 4**. $IC_{50}$ values of sub-fractions and standards in enzyme inhibition and antioxidant assays.

| Sub-fractions | $IC_{50}$ (µg/mL) | | | |
|---|---|---|---|---|
| | α-Glucosidase | α-Amylase | DPPH scavenging | Metal chelating |
| SF1 | 102.80±04.10 | 117.10±11.21 | 152.67±17.03 | 250.23±11.18 |
| SF2 | 108.28±13.00 | 202.14±15.19 | 106.78±03.92 | 169.78±12.15 |
| SF3 | 99.78±17.25 | 137.55±19.61 | 163.31±11.08 | 197.17±10.50 |
| SF4 | 89.03±09.12 | 95.84±11.45 | 103.62±3.03 | 109.86±06.80 |
| SF5 | **19.54±01.05** | **23.84±02.42** | **28.63±01.78** | **21.87±01.92** |
| SF6 | 78.20±02.02 | 82.48±09.45 | 66.23±82.38 | 82.53±09.20 |
| Acarbose | 17.82±01.01 | 21.43±01.05 | - | - |
| Ascorbic Acid | - | - | 37.87±01.01 | - |
| EDTA | - | - | - | 29.12±02.31 |

The FTIR spectrum analysis of SF5 (Table 5) revealed distinct absorption bands corresponding to various functional groups, indicating a complex mixture of bioactive compounds. The FTIR spectrum showed a broad absorption around 3249 $cm^{-1}$, which can be attributed to O–H stretching associated with alcohols and phenolic compounds. A further absorption in the region of 3100 $cm^{-1}$ was consistent with the O–H stretching characteristics of carboxylic acids. The band observed at 2121 $cm^{-1}$ was assigned to C≡N stretching, indicating the possible occurrence of nitrile-containing constituents, including some alkaloidal compounds.

Absorption bands were observed at 1694 and 1693 $cm^{-1}$, consistent with C=O stretching. They may indicate carbonyl-containing compounds, such as esters, ketones, or lactones. Bands at 1618 and 1586 $cm^{-1}$ fall within the range associated with C=C stretching in aromatic structures. Bands appearing at 1469 and 1447 $cm^{-1}$ were attributed mainly to the bending vibrations of $–CH_2$ and $–CH_3$ groups. In addition, the absorption at 1238 $cm^{-1}$ was consistent with C–O–C stretching, indicating the presence of ether linkages within the constituents of the fraction. Overall, the FTIR profile confirms the presence of alcohols, acids, esters, ketones, aromatics, and ethers, supporting the existence of phenolic, flavonoid, and other phytochemical constituents responsible for the bioactivity of the sample.

**Table 5**. FTIR absorption peaks, functional groups, and corresponding classes of compounds.

| Peak ($cm^{-1}$) | Functional Group | Class of Compounds |
|---|---|---|
| **3249** | –OH (stretching) | Alcohol |
| **3100** | –OH (stretching) | Carboxylic acid |
| **2121** | –C≡N (stretching) | Nitrile |
| **1694** | –C=O (stretching) | Ester |
| **1693** | –C=O (stretching) | Ketone |
| **1618** | –C=C (stretching) | Alkene |

| | | |
|---|---|---|
| **1586** | Aromatic C=C (stretching) | Aromatic compounds |
| **1469** | –$CH_2$ (bending) | Methylene |
| **1447** | –$CH_3$ (bending) | Methyl |
| **1238** | –C–O–C (stretching) | Ether |

Figure 1 shows the LC-MS chromatogram of SF5. Multiple peaks appeared at different retention times, indicating several components in the fraction. Retention time is plotted on the horizontal axis and detector response on the vertical axis. Each peak represents a component detected during the separation.

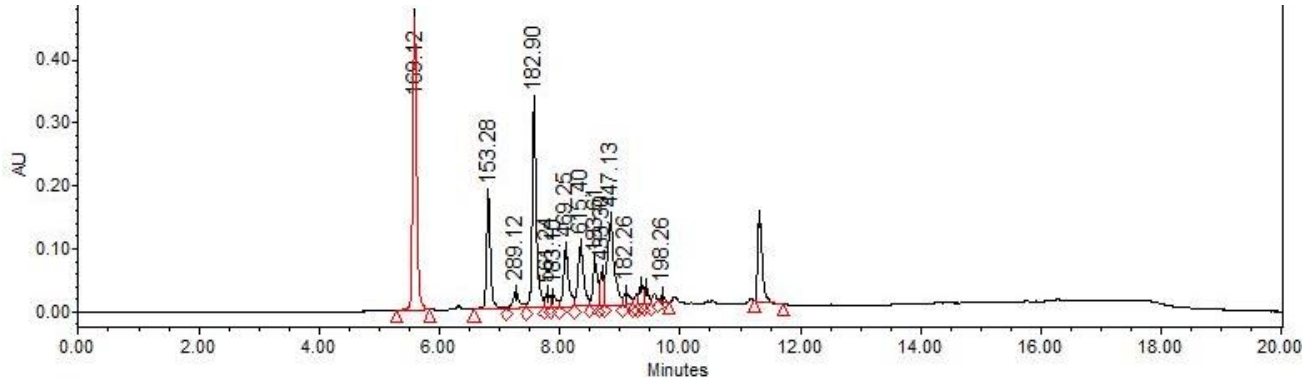



**Figure 1**. Chromatogram of LC-MS analysis of SF5

The LC-MS analysis of the *Anacardium occidentale* leaf fraction (SF5) identified several bioactive phytochemicals (Table 6), highlighting its rich polyphenolic and flavonoid composition. The LC-MS analysis of SF5 revealed several compounds belonging mainly to the phenolic acid, flavonoid and triterpenoid classes. Gallic acid (m/z 169.12) and protocatechuic acid (m/z 153.28) were detected among the phenolic constituents, while methyl gallate (m/z 182.90) was also identified. Other compounds detected included methyl ursolate (m/z 469.25), quercetin-3-O-arabinoside (m/z 433.30), luteolin-7-O-glucoside (m/z 447.13) and amentoflavone (m/z 537.63). The LC-MS profile therefore indicates that SF5 contains a diverse mixture of phenolic acids, flavonoid glycosides and triterpenoid constituents, which may contribute to the biological activities observed for the fraction. The compounds identified from SF5 are presented in Table 6.

**Table 6**. Compounds Identified by LC-MS Analysis of SF5

| Retention Time (min) | Base Peak (m/z), negative mode (M-H) | Exact compound Mass | Identified Compound Through LC-MS |
|---|---|---|---|
| **5.584** | 169.12 | 170.12 | Gallic acid |
| **6.811** | 153.28 | 154.30 | Protocatechuic acid |
| **7.5711** | 182.90 | 183.90 | Methyl gallate |
| **8.097** | 469.25 | 470.10 | Methyl ursolate |
| **8.702** | 433.30 | 434.30 | Quercetin-3-O-arabinoside |
| **8.847** | 447.13 | 448.50 | Luteolin-7-O-glucoside |
| **9.706** | 537.63 | 538.60 | Amentoflavone |

A search of the MassBank database (https://massbank.eu/) identified the following compounds as matching the observed base peaks: gallic acid, protocatechuic acid, methyl gallate, ursolic acid methyl ester, quercetin-3-O-arabinoside, luteolin-7-O-glucoside, and amentoflavone (Table 6). Figure 2 shows the structures of these compounds.

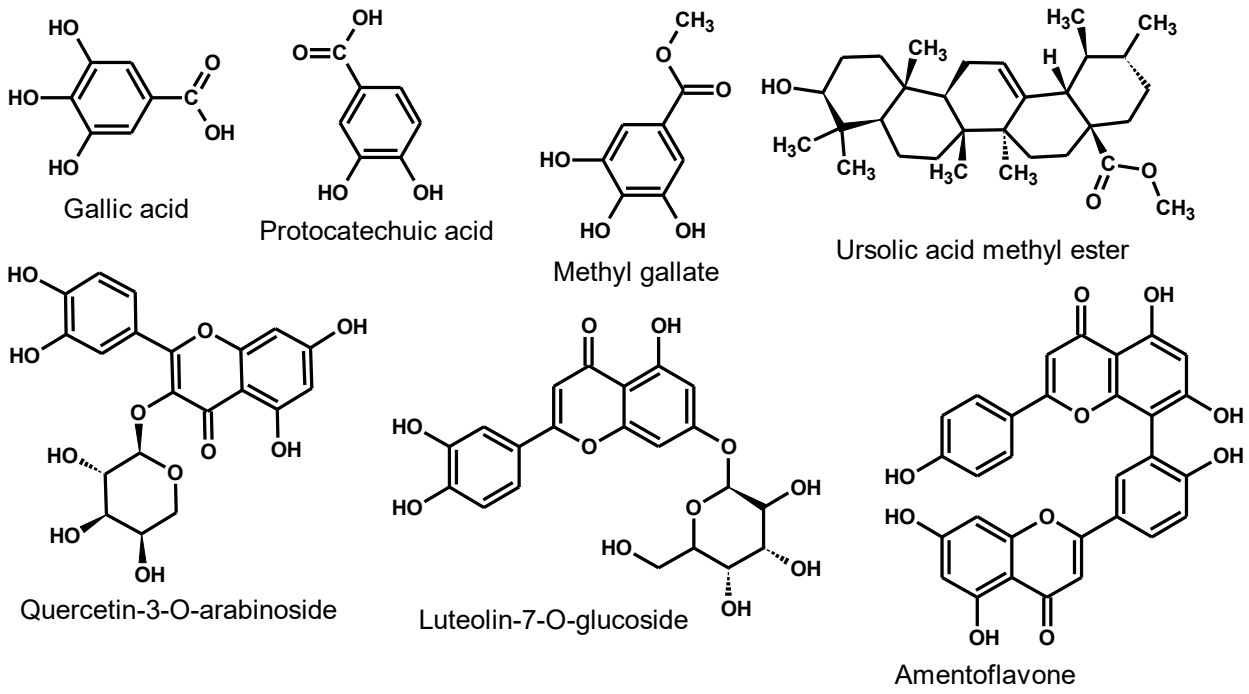



**Figure 2**. Structures of the Identified Compounds

The inhibitory potential of the compounds shown in Figure 2 was evaluated by molecular docking. As shown in Table 7, docking results revealed varying binding affinities (kcal/mol) of SF5 phytochemicals with $\alpha$-amylase, $\alpha$-glucosidase, and heme oxygenase-1 (HO-1). Amentoflavone interacted with all three target proteins, giving binding energies of −7.11, −6.60 and −7.11 kcal/mol, respectively. Luteolin-7-O-glucoside and quercetin-3-O-arabinoside also produced relatively favorable docking scores, with values of −7.26 and −7.03 kcal/mol, respectively, particularly in their interactions with HO-1. Methyl ursolate showed binding energies ranging from −6.99 to −6.24 kcal/mol across the evaluated targets. In contrast, the phenolic acids and methyl gallate produced less favourable scores, with gallic acid, protocatechuic acid and methyl gallate generally falling within the range of approximately −4.0 to −4.6 kcal/mol.

For comparison, the reference compounds acarbose and zinc protoporphyrin produced binding energies of −8.48 and −7.09 kcal/mol for the respective enzyme targets and −7.81 kcal/mol for HO-1. The docking scores obtained for amentoflavone and luteolin-7-O-glucoside were within a similar range to those observed for the reference compounds. Overall, the docking results indicate that several constituents detected in SF5 were capable of interacting with the selected antidiabetic and antioxidant targets, with amentoflavone, luteolin-7-O-glucoside, and quercetin-3-O-arabinoside showing comparatively favorable binding profiles.

**Table 7**. Docking Scores of Identified Compounds with $\alpha$-Amylase, $\alpha$-Glucosidase, and Heme Oxygenase-1 (HO-1)

| PubChem CID | Tentative compound | Docking Score (kcal/mol) | | |
|---|---|---|---|---|
| | | $\alpha$-Amylase | $\alpha$-Glucosidase | HO-1 |
| **370** | Gallic acid | -4.0892 | -4.4528 | -4.6655 |
| **72** | Protocatechuic acid | -4.0261 | -4.3463 | -4.4373 |

| | | | | |
|---|---|---|---|---|
| **7428** | Methyl gallate | -4.5286 | -4.5775 | -4.4708 |
| **636516** | Methyl ursolate | -6.9872 | -5.7129 | -6.2402 |
| **12309865** | Quercetin-3-O-arabinoside | -6.2652 | -6.0197 | -7.0287 |
| **45933934** | Luteolin-7-O-glucoside | -6.9139 | -6.1219 | -7.2579 |
| **5281600** | Amentoflavone | -7.1133 | -6.6014 | -7.1090 |
| **9811704** | Acarbose (Reference Ligand) | -8.4760 | -7.0948 | - |
| **71312673** | ZnPP (Reference Ligand) | - | - | -7.8112 |

Figures 3-8 illustrate the molecular docking interactions between the top-performing ligands and their target enzymes, showing how these compounds occupy the active sites and form stabilizing bonds. The docking poses for α-amylase are presented in Figures 3 and 4. Acarbose established several hydrogen-bonding and hydrophobic contacts within the binding site, whereas amentoflavone adopted a comparable orientation and formed hydrogen-bond and π–π interactions with residues in the same region.

Figures 5 and 6 show acarbose and amentoflavone docked in the catalytic region of α-glucosidase. Both compounds formed hydrogen bonds and aromatic interactions with the enzyme. Figures 7 and 8 show the docked compounds in HO-1. Zn protoporphyrin (ZnPP) formed π interactions and coordinated with the heme region, while luteolin-7-O-glucoside sat near the heme group and formed hydrogen bonds and π–π contacts.

**Pictorial Docking Results**

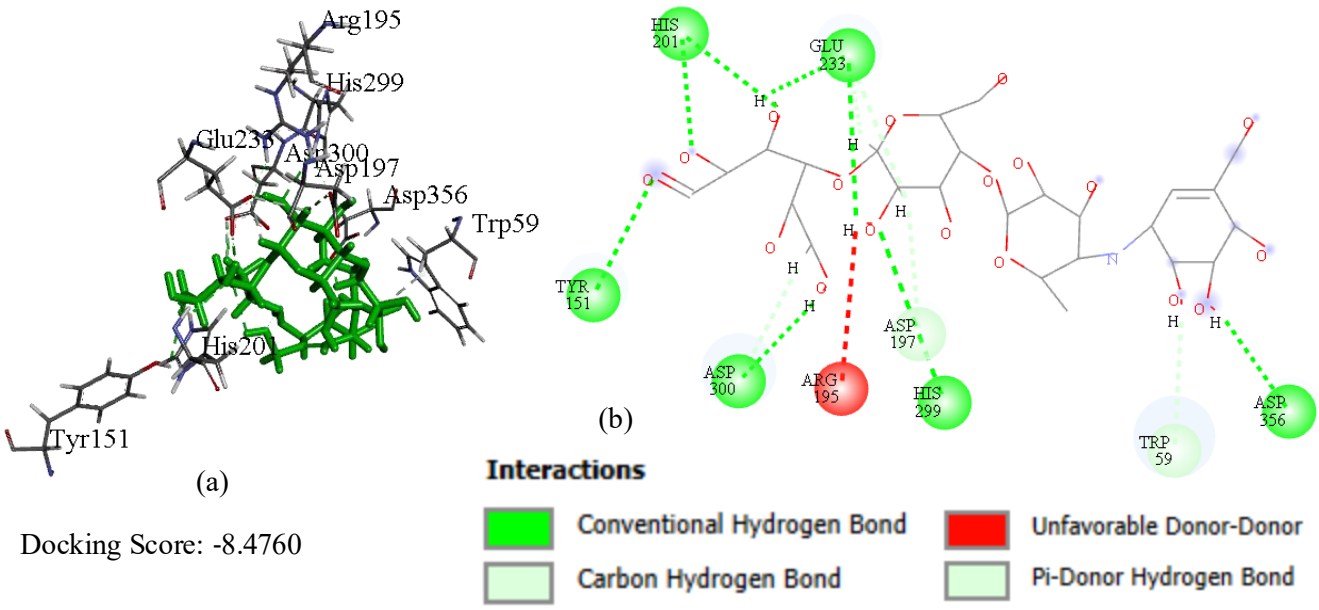



**Figure 3**. Illustration of the interaction between α-amylase side chains and Acarbose (Standard Reference) presented in (a) three-dimensional and (b) two-dimensional formats.

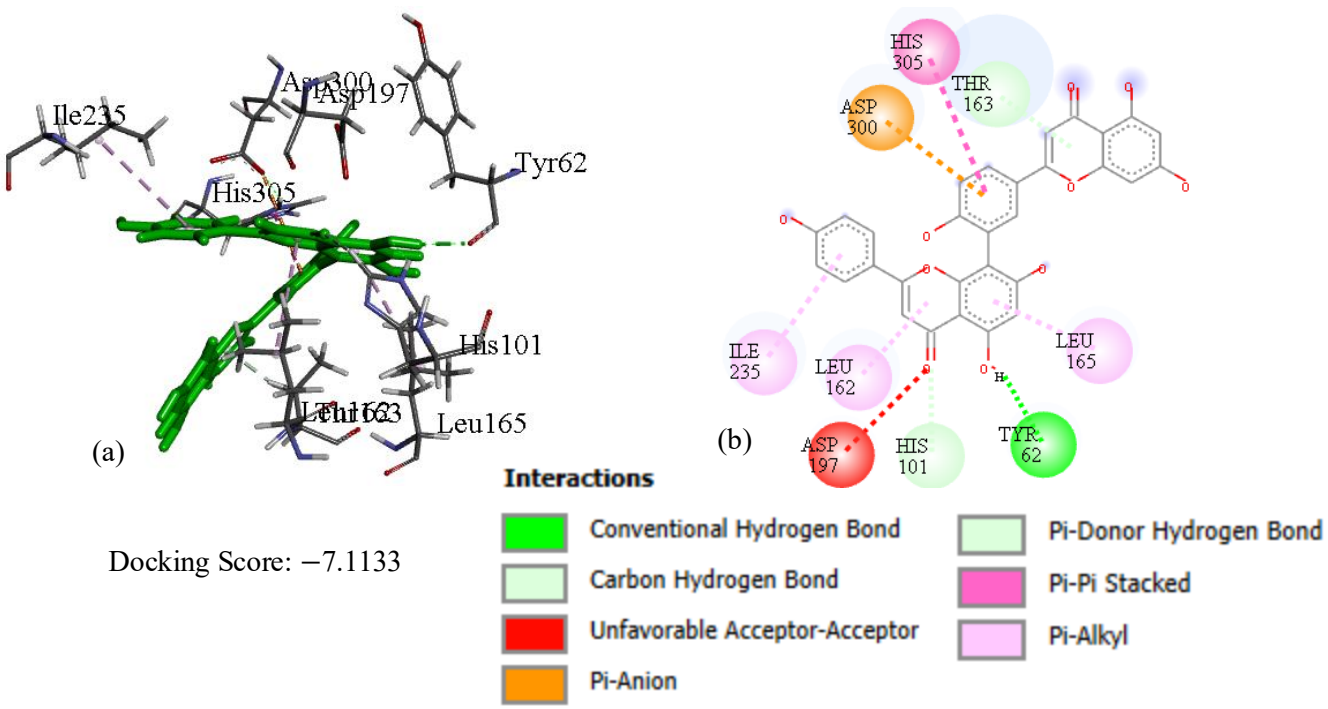



**Figure 4**. Illustration showing the interaction between $\alpha$-amylase side chains and Amentoflavone in (a) 3D and (b) 2D formats.

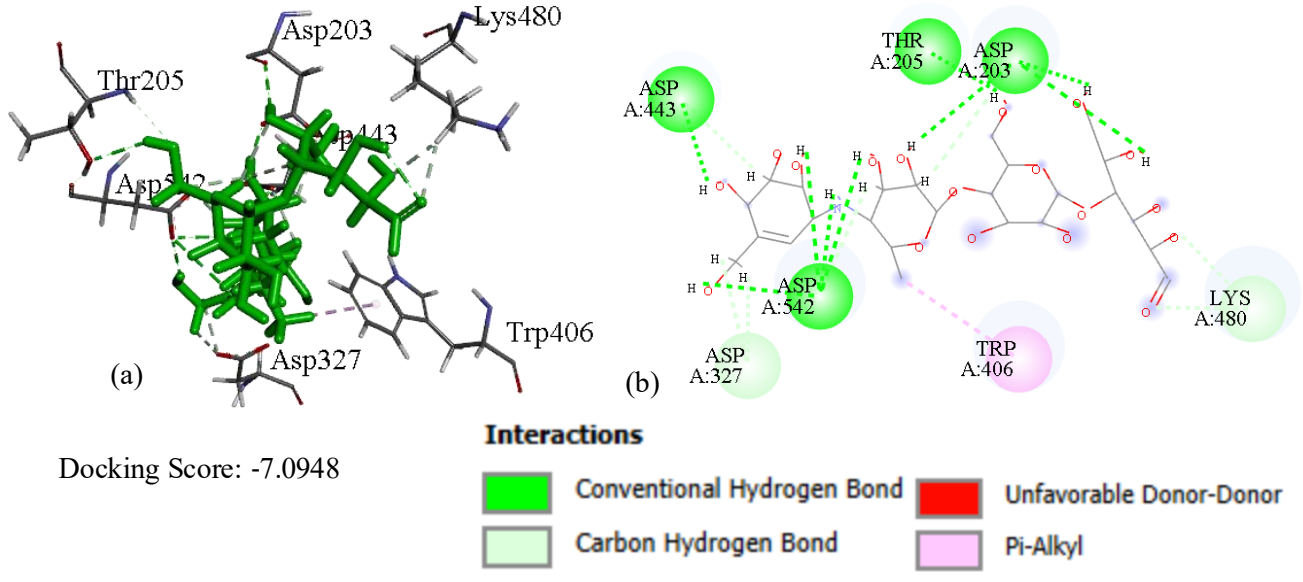



**Figure 5**. Illustration of the interaction between the side chains of alpha-glucosidase and acarbose (standard reference), shown in (a) three-dimensional and (b) two-dimensional representations.

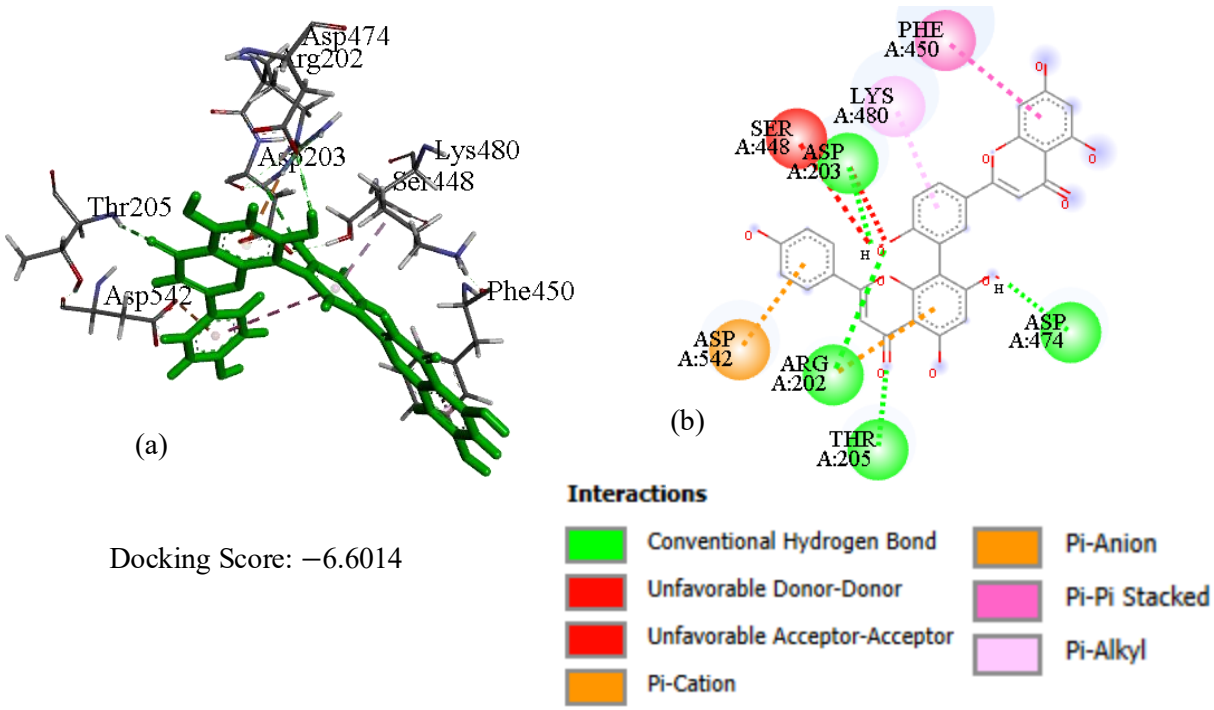



**Figure 6**. Depiction of how the side chains of alpha-glucosidase interact with Amentoflavone, shown in both (a) three-dimensional and (b) two-dimensional representations.

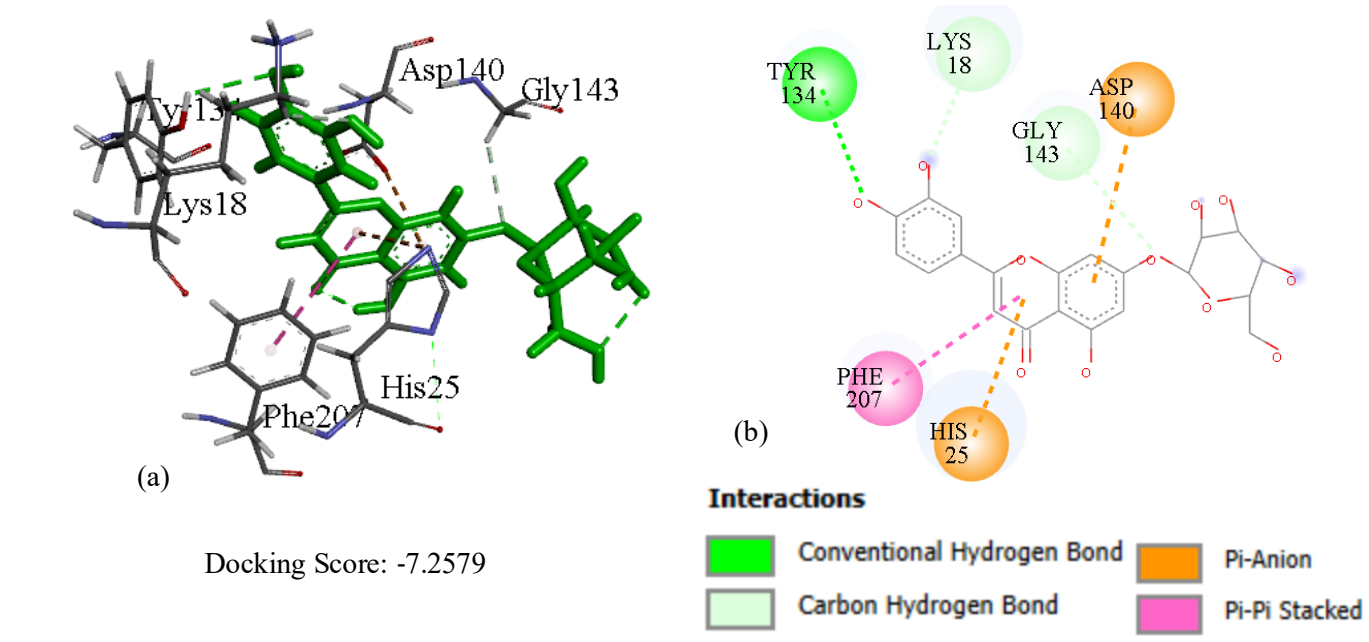



**Figure 7**. A depiction of how the side chains of Heme oxygenase-1 (HO-1) interact with Luteolin-7-O-glucoside, shown in both three-dimensional and two-dimensional views.

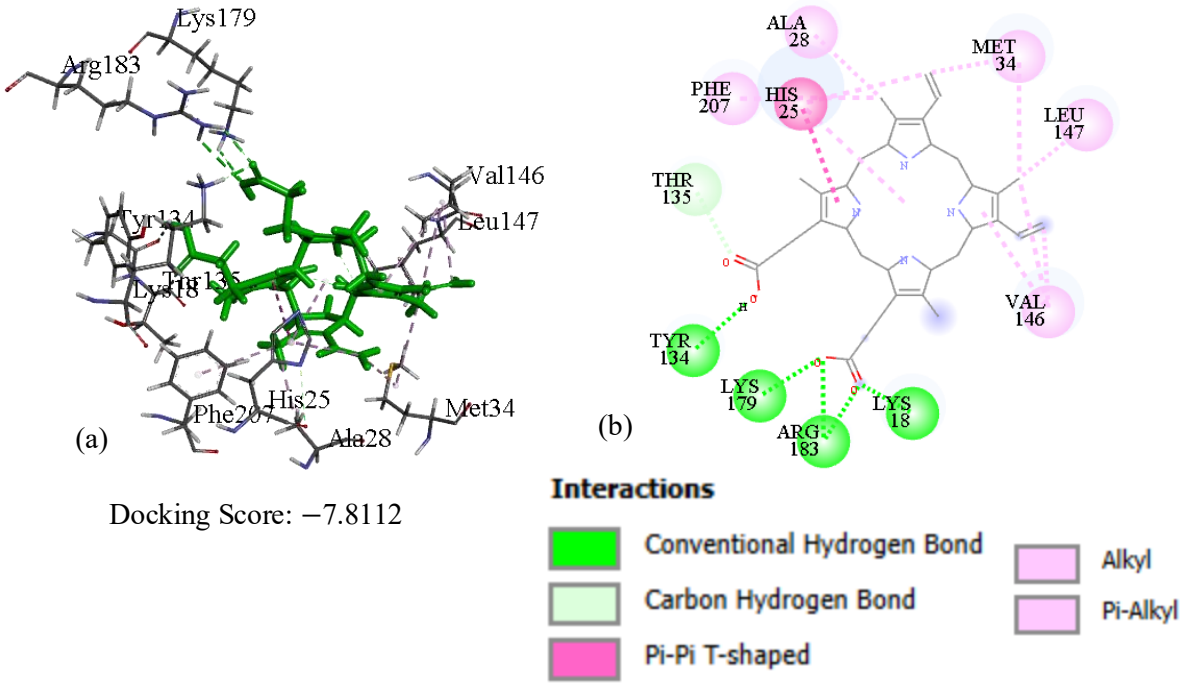



**Figure 8**. Depiction of the interactions between the side chains of Heme oxygenase-1 (HO-1) and Zinc Protoporphyrin (ZnPP) (the standard reference), shown in both three-dimensional and two-dimensional views.

Table 8 presents the molecular interactions predicted for the principal SF5 constituents and the reference ligands at the α-amylase, α-glucosidase and haem oxygenase-1 (HO-1) binding sites. Within α-amylase, amentoflavone was associated with a hydrogen bond involving Tyr62, π–π stacking with His305, and π–alkyl contacts involving Leu162 and Leu165. Luteolin-7-O-glucoside was positioned in the same binding region and showed hydrogen-bond interactions with His299 and Asn298, together with a π–anion contact involving Glu233. The reference ligand, acarbose, established several hydrogen bonds, including contacts with His201, Glu233 and Asp300.

The α-glucosidase complexes showed hydrogen-bond contacts between amentoflavone and Asp203, Arg202 and Thr205, accompanied by π–π stacking with Phe450. Luteolin-7-O-glucoside was associated with Asp443 through hydrogen-bond and π–anion interactions. Acarbose also occupied the catalytic region, with contacts involving Asp203, Asp443 and Asp542.

In the HO-1 binding region, amentoflavone formed a hydrogen bond with Tyr134 and a π–π interaction with Phe207. Luteolin-7-O-glucoside formed a hydrogen bond with Arg183 and a π–π interaction with His25.

**Table 8**. Comparative Molecular Interaction Patterns of SF5 Bioactive Compounds and Reference Ligands at the Active Sites of α-Amylase, α-Glucosidase, and HO-1

| S/N | Components of SF5 | Interactions and Types | | |
|---|---|---|---|---|
| | | Alpha-Amylase | Alpha-Glucosidase | Heme Oxygenase-1 (HO-1) |
| **1.** | Amentoflavone | **H-Bond:** Tyr62<br>**C-H/π-Donor-H Bond:** His101, Thr163,<br>**π-π Stacked:** His305<br>**π-Alkyl:** Ile235, Leu162, Leu165<br>**π-Anion:** Asp300 | **H-Bond:** Asp203, Arg202, Thr205, Asp474<br>**π-Cation/π-Anion:** Asp542, Arg202<br>**π-π Stacked:** Phe450<br>**π-Alkyl:** Lys480 | **H-Bond:** Arg183, Tyr134, Gln38, Glu29<br>**van der Waals:** Asp140, Gly143<br>**C-H:** Gly139<br>**π-S:** Met34<br>**π-π T-Shaped/ Amide-π Stacked/π-Alkyl:** Leu138, Ser142, Gly139, His25 |
| **2.** | Luteolin-7-O-glucoside | **H-Bond:** His299, Asn298, His201<br>**C-H:** Asp300<br>**π-Anion:** Glu233<br>**π-Alkyl:** Leu165 | **H-Bond:** Asp443<br>**C-H:** Asp542<br>**π-Anion:** Asp203 | **H-Bond:** Tyr134<br>**C-H:** Lys18, Gly143<br>**π-Anion:** Asp140, His25<br>**π-π Stacked:** Phe207 |
| **3.** | Acarbose (Standard Reference) | **H-Bond:** His201, Glu233, Tyr151, Asp300, His299, Asp356<br>**C-H/π-donor-H Bond:** Asp197, Trp59, Asp300 | **H-Bond:** Asp443, Thr205, Asp203, Asp542<br>**C-H:** Asp327, Lys480<br>**π-Alkyl:** Trp406 | - |
| **4.** | Zinc Protoporphyrin (ZnPP) (Standard Reference) | - | - | **H-Bond:** Tyr134, Lys179, Arg183, Lys18<br>**C-H:** Thr135<br>**π-π T-Shaped:** His25<br>**Alkyl/π-Alkyl:** Phe207, Ala28, Met34, Leu147, Val146 |

### 3.2. Discussion

The present study evaluated the bioactivities of fractions and sub-fractions derived from the MEAOL, with particular emphasis on their inhibitory effects against α-amylase and α-glucosidase, as well as their antioxidant activities. These findings were further supported by structural characterization using FTIR and LC-MS analyses, together with in silico molecular docking of the identified compounds.

**Enzyme Inhibition Potential**

Among the pooled fractions, PF5 showed the strongest activity with the lowest $IC_{50}$ values against α-glucosidase and α-amylase. Following PTLC separation, SF5 had the lowest $IC_{50}$ values against the two enzymes. This increase in activity suggests that PTLC concentrated compounds that inhibit these enzymes in SF5. Acarbose was more active than SF5, which inhibited both enzymes involved in carbohydrate digestion. Similar activity has been reported for solvent fractions of *Anacardium occidentale* (Lawal et al., 2026). The constituents of SPF5 may be useful to curb the menace of diabetes mellitus (Konare et al., 2024). These findings warrant further study of compounds in *Anacardium occidentale* leaves that may inhibit these enzymes (Pham et al., 2023).

**Antioxidant Potential**

Among the subfractions, SF5 showed the most potent for DPPH radical-scavenging and metal-chelating activity by having the least $IC_{50}$ respectively. Their $IC_{50}$ values are close to those of ascorbic acid and EDTA respectively. These suggest that SF5 act as both radical scavenging and metal chelation. These mechanisms are useful in oxidative processes linked to diabetes and its complications

(Elekofehinti et al., 2016). This is because excess reactive oxygen species and metal-mediated reactions can contribute to cellular damage (Lawal et al., 2026).

Antioxidant activity has also been reported in polyphenol-rich *Anacardium* extracts (Sassi et al., 2019). Flavonoids, tannins, and other phenolic compounds in these fractions have been linked to radical scavenging and other antioxidant effects (Belgis, 2024). The activity of SF5 may therefore be associated with the phenolic and flavonoid constituents detected in the fraction (Pham et al., 2023).

**Structural Characterization**

The FTIR spectrum of SF5 contained bands associated with hydroxyl, carbonyl, ether, and aromatic groups (Mabasa et al., 2021). These groups are found in plant metabolites such as phenolic acids, flavonoids (Krysa et al., 2022), and terpenoids (Wongsa et al., 2022). LC-MS analysis tentatively identified gallic acid, protocatechuic acid, methyl gallate, quercetin-3-O-arabinoside, luteolin-7-O-glucoside, amentoflavone, and methyl ursolate. Most of these compounds have been reported in contributing to oxidative stress amelioration and lowering postprandial hyperglycemia (Chen et al., 2022). Phenolic acids and flavonoids have been reported to have contributed to antioxidant effects (Corkovic et al., 2022) and inhibition of carbohydrate-digesting enzymes (Kim et al., 2000). Some of these compounds have also been linked to the Nrf2/HO-1 antioxidant pathway (Feng et al., 2018; Marino et al., 2014). Gallic acid, one of the phenolic acids detected in SF5, has previously been reported to inhibit both $\alpha$-glucosidase and $\alpha$-amylase. Studies have also indicated that gallic acid can act in combination with other inhibitors to enhance carbohydrate-digestive enzyme inhibition (Oboh et al., 2016). Its detection in SF5 may therefore contribute to the enzyme-inhibitory activity observed in the present study. In addition to its potential role in enzyme inhibition, gallic acid possesses antioxidant properties that have been linked to its ability to donate hydrogen atoms and interact with reactive species (Marino et al., 2014). Experimental evidence has further associated gallic acid with modulation of Nrf2/HO-1-related antioxidant responses (Feng et al., 2018), providing a possible explanation for some of the antioxidant effects associated with gallic acid-containing plant fractions.

Protocatechuic acid, which was detected in SF5, has been reported to have antidiabetic and antioxidant effects. Ding et al. (2024) reported that it inhibits $\alpha$-glucosidase and lowers postprandial blood glucose. Protocatechuic acid has also been identified alongside gallic acid in activity-guided studies of antidiabetic plant extracts (Alegbe et al., 2019). Report has also found that protocatechuic acid can scavenge radicals, chelate metals, and act as a reducing agent (Li et al., 2011). Presence of protocatechuic acid in SF5 may have contributed to the antidiabetic and antioxidant activities observed in SF5. Methyl gallate and other galloyl esters have been identified in plant extracts that inhibit $\alpha$-glucosidase and $\alpha$-amylase (Ahmed et al., 2024). Alkyl gallates have also been reported to scavenge reactive species (Domínguez-Perles et al., 2023). Presence of methyl gallate in SF5 may therefore contribute to the enzyme-inhibitory and antioxidant activity observed. Methyl ursolate, pentacyclic triterpenoid, is related to ursolic acid. Ursolic acid and other ursane-type triterpenoids have been associated with antidiabetic effects (Bakry et al., 2025). Presence of triterpenoids in SF5 may also affect oxidative processes and pathways involved in insulin responsiveness (Seo et al., 2018).

It has been reported that Flavones and flavonols can inhibit $\alpha$-glucosidase and $\alpha$-amylase, but their activity varies with chemical structure (Lam et al., 2024). The positions of hydroxyl groups and the presence of sugar groups can affect enzyme inhibition. Glycosylated flavonoids may bind less strongly to these enzymes than their aglycones (Lam et al., 2024). Luteolin has shown inhibitory activity against both enzymes (Kim et al., 2000). Luteolin-7-O-glucoside and quercetin-3-O-arabinoside, which were detected in SF5, may also contribute to its activity, though their sugar groups could affect how they interact with the enzymes. Luteolin- and quercetin-derived compounds may also influence cellular antioxidant responses (Luo et al., 2019), including pathways involving Nrf2 and HO-1 (Sun et al., 2012).

Amentoflavone, a biflavonoid detected in SF5, has been reported to inhibit $\alpha$-amylase and $\alpha$-glucosidase (Li et al., 2023). Its aromatic rings and oxygen-containing groups may interact with the enzymes' binding sites (Jurcevic et al., 2023). Amentoflavone has also been associated with antioxidant and anti-inflammatory activities and has been investigated in relation to Nrf2/HO-1-mediated cellular responses (Rong et al., 2022). In the present study, its detection in SF5, together with its favorable docking profiles across the selected targets, suggests that amentoflavone may be one of the constituents contributing to the observed enzyme-inhibitory and antioxidant activities. Nevertheless, the activity of SF5 is likely to reflect the combined effects of several constituents rather than the action of a single compound.

**Molecular Docking Analysis and Predicted Molecular Interactions**

Docking results help explain the biological activity of SF5 at the molecular level. The compounds differed in their docking scores and in the residues they contacted within the target proteins. Amentoflavone, luteolin-7-O-glucoside, and quercetin-3-O-arabinoside showed favorable interactions with the selected targets. The docking results therefore suggest that several constituents of SF5 may have the capacity to associate with regions of the proteins involved in their biological functions.

Amentoflavone docking scores are consistent with the research of Li et al., (2023), and Lam et al., (2024) that biflavonoid compounds inhibit $\alpha$-amylase and $\alpha$-glucosidase. Luteolin-7-O-glucoside and quercetin-3-O-arabinoside also had favorable docking scores against the target proteins. Luteolin-7-O-glucoside formed hydrogen bonds with His299 and Asn298 and a $\pi$–anion interaction with Glu233 in $\alpha$-amylase. In $\alpha$-glucosidase, it interacted with Asp443. The attached sugar groups affect the size of the flavonoids, polarity, solubility, and access to hydrophobic regions of the enzymes. Their effect on inhibitory activity depends on the parent flavonoid and the position of the sugar group (Lam et al., 2024). Sugar hydroxyl groups may also form hydrogen bonds with residues in the binding pocket.

Gallic acid, protocatechuic acid, and methyl gallate had less favorable docking scores than the larger flavonoids, possibly because their smaller structures form fewer hydrophobic and aromatic contacts in the binding sites (Oboh et al., 2016). However, it has been reported that docking scores alone do not establish whether a compound is biologically active. Phenolic compounds, especially in polyphenol-rich extracts, have been reported to inhibit $\alpha$-amylase and $\alpha$-glucosidase (Pan et al., 2025). Phenolic acids can also scavenge radicals, donate hydrogen, bind metal ions (Chen et al., 2022), and participate in reduction reactions (Li et al., 2011). The HO-1 docking results suggest a possible basis for SF5 antioxidant activity. Many of the identified compounds docked near the heme-associated region. Report has shown that flavonoids and other polyphenols also support cellular antioxidant defenses through the Nrf2/ARE pathway (Huang et al., 2023). This can increase HO-1 and other protective proteins (Suraweera et al., 2020).

## 4. CONCLUSION

In conclusion, the sterile $dH_20$ Cold fresh Tiger nut extract, sterile $dH_20$ Hot fresh Tiger nut extract and Sterile $dH_20$ Hot dried Tiger nut extracts in this study exhibited a broad-spectrum antibacterial activity on *Staphylococcus aureus, Escherichia coli* and *Morganella morganii* with highest activity recorded for sterile $dH_20$ Cold fresh Tiger nut extract. This may be attributed to its vast concentration of phytochemical compounds. More research should be carried out on tiger nuts for comprehensive structural elucidation of bioactive compounds in order to formulate a new drug to treat infections.

While benefits of tiger nuts are countless it is also worth noting that there are some side effects, too, mainly skin allergies, respiratory reactions and gastrointestinal issues. Those suffering from any disorder need proper diagnosis. Use tiger nuts (and other natural remedies) wisely, only with prior consent of a physician. Medicines derived from plants have made potent and effective contribution towards the treatment and healing of humans and act as a source of research focus for novel drug compounds.

Tiger nut is cheap, unexploited, and eaten without much knowledge of its benefits; hence we recommend an urgent need for awareness campaigns on its health and nutritional benefits. There is scanty information on tiger nut metabolites bioavailability, this area needs to be explored through various approaches including in vivo studies. Promoting tiger nut consumption will play a role in the health, nutrition and economy of some developing countries where this tuber is grown.

**LIST OF ABBREVIATIONS**

2D: Two-Dimensional
3D: Three-Dimensional
CID: Compound identification number
DNSA: 3,5-Dinitrosalicylic acid
HO-1: Heme Oxygenase-1
SF5: Subfraction 5
$R_f$: Retardation factor
MEAOL: Methanol extract of *Anacardium occidentale* leaves
$IC_{50}$: Inhibitory concentration for 50% reduction in activity
LC: Liquid Chromatography
LC-MS: Liquid Chromatography Mass Spectrometry

MOE: Molecular Operating Environment
MS: Mass Spectrometry
PDB: Protein Data Bank
pNPG: p-nitrophenyl-β-D-glucopyranoside
DPPH: 2,2-Diphenyl-1-picrylhydrazyl
FTIR: Fourier Transform Infrared Spectroscopy
EDTA: Ethylenediaminetetraacetic Acid
PTLC: Preparative Thin Layer Chromatography
MDB: Molecular Database
RMSD: Root Mean Square Deviation
PTFE: Polytetrafluoroethylene
ZnPP: Zinc Protoporphyrin IX

**Acknowledgements**
The authors of this article would like to express gratitude to Mallam Haruna Tsoho Bala from the Biochemistry Department at Bayero University Kano (BUK) for his support in laboratory investigative activities. Additionally, thanks are extended to Dr. Bashir Musa from the Centre for Dryland Agriculture at BUK, Nigeria, for his assistance with the LC-MS analysis during this research.

**Author Contributions:**
The author made substantial contributions to the conception and design of the study, its execution, data collection, analysis, and interpretation of the findings. The author approved the final version of the manuscript for publication, consented to its submission to the selected journal, and accepted responsibility for all aspects of the work, including ensuring its accuracy and integrity.

**Ethical Approval**
In this article, as per the plant regulations followed in the Biochemistry and Forensic Science Department, Faculty of Science, Nigeria Police Academy, Wudil, Kano, Nigeria; the authors observed the *In Vitro* Evaluation and Molecular Docking Studies of α-Glucosidase and α-Amylase Inhibitory and Antioxidant Activities of *Anacardium occidentale* Leaves. The ethical guidelines for plants & plant materials are followed in the study for plant observation, identification & experimentation. This article does not contain any studies with human participants or animals performed by any of the authors.

**Informed Consent**
Not applicable.

**Conflicts of interests**
The authors declare that they have no conflicts of interest, competing financial interests or personal relationships that could have influenced the work reported in this paper.

**Funding**
This research was funded by the Tertiary Education Trust Fund (TETFund) under grant number: TETF/DR&D/CE/UNIV/WUDIL/IBR/2024VOL.I

**Data and materials availability**
Data that support the findings of this study are embedded within the manuscript.

## REFERENCES

1. Ahmed ZB, Mahammed TH, Chegma T, Seidel V, Yousfi M. Alpha-glucosidase and α-amylase inhibitory activity of Pistacia atlantica Desf. gall extracts and identification of putative bioactives using a combined UPLC fingerprinting and molecular docking approach. Journal of Diabetes &

Metabolic Disorders 2024;23(2):2081–2094. doi: https://doi.org/10.1007/s40200-024-01470-y.

2. Alegbe EO, Teralı K, Olofinsan KA, Surgun S, Ogbaga CC, Ajiboye TO. Antidiabetic activity-guided isolation of gallic and protocatechuic acids from Hibiscus sabdariffa calyxes. Journal of Food Biochemistry 2019;43(7):e12927. doi: https://doi.org/10.1111/jfbc.12927.
3. Ali A, Cottrell JJ, Dunshea FR. Antioxidant, alpha-glucosidase inhibition activities, in silico molecular docking and pharmacokinetics study of phenolic compounds from native Australian fruits and spices. Antioxidants 2023;12(2):254. doi: https://doi.org/10.3390/antiox12020254.
4. Assefa ST, Yang EY, Chae SY, Song M, Lee J, Cho MC, Jang S. Alpha glucosidase inhibitory activities of plants with focus on common vegetables. Plants 2020;9(1):2. doi: https://doi.org/10.3390/plants9010002.
5. Bakry SM, El-Shiekh RA, Hatem S, Mandour AA, El-Dessouki AM, Bishr A, Elosaily H, Mohamed AF, Elhusseiny SM. Therapeutic applications of ursolic acid: A comprehensive review and utilization of predictive tools. Future Journal of Pharmaceutical Sciences 2025;11(1):48. doi: https://doi.org/10.1186/s43094-025-00796-5.
6. Baliyan S, Mukherjee R, Priyadarshini A, Vibhuti A, Gupta A, Pandey RP, Chang CM. Determination of antioxidants by DPPH radical scavenging activity and quantitative phytochemical analysis of Ficus religiosa. Molecules 2022;27(4):1326. doi: https://doi.org/10.3390/molecules27041326.
7. Belgis B. Phytochemical screening and antioxidant activity of phenolic compound from Anacardium occidentale leaf extract. Jurnal Medika Nusantara 2024;2(2):1–7. doi: https://doi.org/10.59680/medika.v2i2.983.
8. Chen J, Huang Z, Cao X, Chen X, Zou T, You J. Plant-derived polyphenols as Nrf2 activators to counteract oxidative stress and intestinal toxicity induced by deoxynivalenol in swine: An emerging research direction. Antioxidants 2022;11(12):2379. doi: https://doi.org/10.3390/antiox11122379.
9. Corkovic I, Pichler A, Simunovic J, Kopjar M. Dietary polyphenols as natural inhibitors of $\alpha$-amylase and $\alpha$-glucosidase. Life 2022;12(11):1692. doi: https://doi.org/10.3390/life12111692.
10. Dej-Adisai S, Rais IR, Wattanapiromsakul C, Pitakbut T. Alpha-glucosidase inhibitory assay-screened isolation and molecular docking model from Bauhinia pulla active compounds. Molecules 2021;26(19):5970. doi: https://doi.org/10.3390/molecules26195970.
11. Ding H, Huang S, Chook CY, Kwek E, Yan C, Ma K, Liu J, Zhu H, Chen ZY. Blood glucose-lowering activity of protocatechuic acid is mediated by inhibiting $\alpha$-glucosidase. Food Science of Human Wellness 2024;13(3):1212–1219. doi: https://doi.org/10.26599/FSHW.2022.9250101.
12. Dirir AM, Daou M, Yousef AF, Yousef LF. A review of alpha-glucosidase inhibitors from plants as potential candidates for the treatment of type-2 diabetes. Phytochemistry Reviews 2022;21(4):1049–1079. doi: https://doi.org/10.1007/s11101-021-09773-1.
13. Domínguez-Perles R, García-Viguera C, Medina S. New anti-$\alpha$-glucosidase and antioxidant ingredients from winery byproducts: Contribution of alkyl gallates. Journal of Agricultural and Food Chemistry 2023;71(40):14615–14625. doi: https://doi.org/10.1021/acs.jafc.3c03759.
14. Elekofehinti OO, Osehodion RO, Adeyelu TT, Ogunwa TH, Olatunde I, Aiwuyo O, Ejelonu OC. Hypoglycemic, hypolipidemic and antioxidant potentials of aqueous and ethanolic leaf extracts of Anacardium occidentale in alloxan induced type I diabetic rat model. Journal of Advances in Medical and Medical Research 2016;14(12):1–10. doi: https://doi.org/10.9734/BJMMR/2016/24357.
15. Encarnacao S, De Mello-Sampayo C, Carrapiço B, São Braz B, Jordão AP, Peleteiro C, Catarino L, Silva IBM da, Gouveia LF, Lima BS, Silva O. Anacardium occidentale bark as an antidiabetic agent. Plants 2022;11(19):2637. doi: https://doi.org/10.3390/plants11192637.
16. Etsassala NGER, Badmus JA, Marnewick JL, Egieyeh S, Iwuoha EI, Nchu F, Hussein AA. Alpha-glucosidase and alpha-amylase inhibitory activities, molecular docking, and antioxidant capacities of Plectranthus ecklonii constituents. Antioxidants 2022;11(2):378. doi: https://doi.org/10.3390/antiox11020378.
17. Feng R, Wang Y, He C, Yang Y, Wan J. Gallic acid, a natural polyphenol, protects against tert-butyl hydroperoxide-induced hepatotoxicity by activating ERK-Nrf2-Keap1-mediated antioxidative response. Food and Chemical Toxicology 2018;119:479–488. doi: https://doi.org/10.1016/j.fct.2017.10.033.
18. Islam WU, Khan F, Waqas M, Ullah S, Halim SA, Rehman NU, Khan H, Mahmoud MH, Batiha GE-S, Khan A, Al-Harrasi A. In-vivo anti-diabetic and anti-hyperlipidemic effects of natural metabolites from resin of Commiphora mukul and their in-silico to in-vitro target fishing. Biomedicine & Pharmacotherapy 2023;165:115214. doi: https://doi.org/10.1016/j.biopha.2023.115214.
19. Jurcevic Sangut I, Sarkanj B, Karalija E, Samec D. A comparative analysis of radical scavenging, antifungal and enzyme inhibition activity of 3′-8″-biflavones and their

monomeric subunits. Antioxidants 2023;12(10):1854. doi: https://doi.org/10.3390/antiox12101854.
20. Kashtoh H, Baek KH. Recent updates on phytoconstituent alpha-glucosidase inhibitors: An approach towards the treatment of type two diabetes. Plants 2022;11(20):2722. doi: https://doi.org/10.3390/plants11202722.
21. Kim JS, Kwon CS, Son KH. Inhibition of alpha-glucosidase and amylase by luteolin, a flavonoid. Bioscience, Biotechnology, and Biochemistry 2000;64(11):2458–2461. doi: https://doi.org/10.1271/bbb.64.2458.
22. Konare MA, Maïga AD, Togola I, Diarra N. Antioxidant and antidiabetic potential of extracts from Anacardium occidentale and Sclerocarya birrea. Journal of Biochemical Technology 2024;15(3):15–24. doi: https://doi.org/10.51847/zpFCZqyBFX.
23. Krysa M, Szymańska-Chargot M, Zdunek A. FT-IR and FT-Raman fingerprints of flavonoids—A review. Food Chemistry 2022;393:133430. doi: https://doi.org/10.1016/j.foodchem.2022.133430.
24. Lam TP, Tran N-V, Pham L-H, Lai V-T, Dang B-T, Truong N-L, Nguyen-Vo S-K, Hoang T-L, Mai T-T, Tran T-D. Flavonoids as dual-target inhibitors against $\alpha$-glucosidase and $\alpha$-amylase: A systematic review of in vitro studies. Natural Products and Bioprospecting 2024;14(1):4. doi: https://doi.org/10.1007/s13659-023-00424-w.
25. Lawal TA, Ononamadu CJ, Akinjoko VO, Segba DE, Sholadoye QO, Bashir M. Evaluation of antioxidant and antidiabetic properties of ethyl acetate fraction from Anacardium occidentale leaves, in-vitro and in-silico. Annals of Pharmaceutical Research 2024;3(2):23–30. doi: https://doi.org/10.51470/APR.2024.03.02.23.
26. Lawal TA, Ononamadu CJ, Okonkwo EK, Adedoyin HJ, Shettima ML, Muhammad IU, Alhassan AJ. In vitro and in vivo hypoglycaemic effect of Camellia sinensis on alpha-glucosidase activity and glycaemic index of white bread. Applied Food Research 2022;2:100037. doi: https://doi.org/10.1016/j.afres.2021.100037.
27. Lawal TA, Sholadoye QO, Adeyemo KA, Segba DE. Antidiabetic and antioxidant potentials of the ethyl acetate fraction of *Momordica charantia* leaf methanolic extract: in vitro and in silico studies. Bioorganic Chemistry 2026;179:110007. doi: https://doi.org/10.1016/j.bioorg.2026.110007.
28. Li H, Yang J, Wang M, Ma X, Peng X. Studies on the inhibition of $\alpha$-glucosidase by biflavonoids and their interaction mechanisms. Food Chemistry 2023;420:136113. doi: https://doi.org/10.1016/j.foodchem.2023.136113.
29. Li X, Wang X, Chen D, Chen S. Antioxidant activity and mechanism of protocatechuic acid in vitro. Functional Foods in Health and Disease 2011;1(7):232–244.
30. Luo M, Tian R, Yang Z, Peng YY, Lu N. Quercetin suppressed NADPH oxidase-derived oxidative stress via heme oxygenase-1 induction in macrophages. Archives of Biochemistry and Biophysics 2019;671:69–76. doi: https://doi.org/10.1016/j.abb.2019.06.007.
31. Mabasa XE, Mathomu LM, Madala NE, Musie EM, Sigidi MT. Molecular spectroscopic (FTIR and UV-Vis) and hyphenated chromatographic (UHPLC-qTOF-MS) analysis and in vitro bioactivities of the Momordica balsamina leaf extract. BioMed Research International 2021;2021:2854217. doi: https://doi.org/10.1155/2021/2854217.
32. Marino T, Galano A, Russo N. Radical scavenging ability of gallic acid toward OH and OOH radicals: Reaction mechanism and rate constants from the density functional theory. The Journal of Physical Chemistry B 2014;118(35):10380–10389. doi: https://doi.org/10.1021/jp505589b.
33. Oboh G, Ogunsuyi OB, Ogunbadejo MD, Adefegha SA. Influence of gallic acid on $\alpha$-amylase and $\alpha$-glucosidase inhibitory properties of acarbose. Journal of Food and Drug Analysis 2016;24(3):627–634. doi: https://doi.org/10.1016/j.jfda.2016.03.003.
34. Oyedemi SO, Oyedemi BO, Ijeh II, Ohanyerem PE, Coopoosamy RM, Aiyegoro OA. Alpha-amylase inhibition and antioxidative capacity of some antidiabetic plants used by the traditional healers in Southeastern Nigeria. The Scientific World Journal 2017;2017:3592491. doi: https://doi.org/10.1155/2017/3592491.
35. Pan G, Lu Y, Wei Z, Li Y, Li L, Pan X. A review on the in vitro and in vivo screening of $\alpha$-glucosidase inhibitors. Heliyon 2024;10(18):e37467. doi: https://doi.org/10.1016/j.heliyon.2024.e37467.
36. Pan J, Nawaz M, Liu J, Liu H, Lv Z, Yang W, Jiao Z, Zhang Q. Exploring synergistic inhibitory mechanisms of flavonoid mixtures on $\alpha$-glucosidase by experimental analysis and molecular dynamics simulation. Food Chemistry 2025;464:141560. doi: https://doi.org/10.1016/j.foodchem.2024.141560.
37. Pham DC, Truong DH, Tran QH, Ho QT, Nguyen TAD, Nguyen TNH, Nguyen TV, Nguyen TTV, Cao TS, Barrow CJ, Nguyen HC. Fractionation, identification of chemical constituents, and biological properties of cashew (*Anacardium occidentale* L.) leaf extracts. Food Science & Nutrition 2023;11(12):7996–8008. doi: https://doi.org/10.1002/fsn3.3718.
38. Piovesana S, Montone CM, Antonelli M, Cavaliere C, La Barbera G, Canepari S, Samperi R, Laganà A, Capriotti AL. Investigation of free seleno-amino acids in extra-virgin olive oil by mixed mode solid phase extraction cleanup and

enantioselective hydrophilic interaction liquid chromatography-tandem mass spectrometry. Food Chemistry 2019;278:17–25. doi: https://doi.org/10.1016/j.foodchem.2018.11.053.

39. Rangel-Galvan M, Pacheco-Hernández Y, Lozoya-Gloria E, Villa-Ruano N. Dietary natural products as inhibitors of $\alpha$-amylase and $\alpha$-glucosidase: An updated review of ligand–receptor correlations validated by docking studies. Food Bioscience 2024;62:105456. doi: https://doi.org/10.1016/j.fbio.2024.105456.
40. Rong S, Yang C, Wang F, Wu Y, Sun K, Sun T, Wu Z. Amentoflavone exerts anti-neuroinflammatory effects by inhibiting TLR4/MyD88/NF-κB and activating Nrf2/HO-1 pathway in lipopolysaccharide-induced BV2 microglia. Mediators of Inflammation 2022;2022:5184721. doi: https://doi.org/10.1155/2022/5184721.
41. Sassi A, Jusoh HM, Bakhtiar MT, Haroun N, Kaderi MA, Rostam MA. Analysis of phenolic content and antioxidant activity in Anacardium occidentale leaves. International Journal of Allied Health Sciences 2019;3(3):830.
42. Seo DY, Lee SR, Heo JW, No MH, Rhee BD, Ko KS, Kwak HB, Han J. Ursolic acid in health and disease. The Korean Journal of Physiology & Pharmacology 2018;22(3):235–248. doi: https://doi.org/10.4196/kjpp.2018.22.3.235.
43. Silva APM da, Silva GS da, Oiram Filho F, Silva MFS, Zocolo GJ, Brito ES de. Structural characterization and in vitro and in silico studies on the anti-$\alpha$-glucosidase activity of anacardic acids from Anacardium occidentale. Foods 2024;13(24):4107. doi: https://doi.org/10.3390/foods13244107.
44. Sun GB, Sun X, Wang M, Ye JX, Si JY, Xu HB, Meng XB, Qin M, Sun J, Wang HW, Sun XB. Oxidative stress suppression by luteolin-induced heme oxygenase-1 expression. Toxicology and Applied Pharmacology 2012;265(2):229–240. doi: https://doi.org/10.1016/j.taap.2012.10.002.
45. Suraweera TL, Vasantha Rupasinghe HP, Dellaire G, Xu Z. Regulation of Nrf2/ARE pathway by dietary flavonoids: A friend or foe for cancer management? Antioxidants 2020;9(10):973. doi: https://doi.org/10.3390/antiox9100973.
46. Wong FC, Yong AL, Ting EP, Khoo SC, Ong HC, Chai TT. Antioxidant, metal chelating, anti-glucosidase activities and phytochemical analysis of selected tropical medicinal plants. Iranian Journal of Pharmaceutical Research 2014;13(4):1409–1415. doi: https://doi.org/10.22037/ijpr.2014.1588.
47. Wongsa P, Phatikulrungsun P, Prathumthong S. FT-IR characteristics, phenolic profiles and inhibitory potential against digestive enzymes of 25 herbal infusions. Scientific Reports 2022;12(1):1–11. doi: https://doi.org/10.1038/s41598-022-10669-z.
48. Yadav AS, Bhatnagar D. Free radical scavenging activity, metal chelation and antioxidant power of some of the Indian spices. BioFactors 2007;31(3–4):219–227. doi: https://doi.org/10.1002/biof.5520310309.